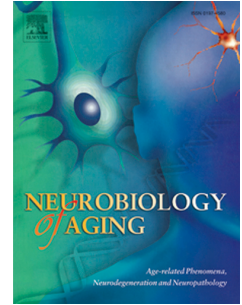# Accepted Manuscript

Unveiling the olfactory proteostatic disarrangement in Parkinson's disease by proteome-wide profiling

Mercedes Lachén-Montes, Andrea González-Morales, Ibon Iloro, Felix Elortza, Isidre Ferrer, Djordje Gveric, Joaquín Fernández-Irigoyen, Enrique Santamaría

Please cite this article as: Lachén-Montes, M., González-Morales, A., Iloro, I., Elortza, F., Ferrer, I., Gveric, D., Fernández-Irigoyen, J., Santamaría, E., Unveiling the olfactory proteostatic disarrangement in Parkinson's disease by proteome-wide profiling, *Neurobiology of Aging* (2018), doi: https://doi.org/10.1016/j.neurobiolaging.2018.09.018.

1   **Unveiling the olfactory proteostatic disarrangement in Parkinson's disease**

2   **by proteome-wide profiling**

3   Mercedes Lachén-Montes,[1,2] Andrea González-Morales,[1,2] Ibon Iloro,[3] Felix Elortza,[3]

4   Isidre Ferrer,[4] Djordje Gveric,[5] Joaquín Fernández-Irigoyen,[1,2]§, Enrique

5   Santamaría,[1,2]§

6

7   *¹ Clinical Neuroproteomics Group, Navarrabiomed, Complejo Hospitalario de Navarra*

8   *(CHN), Universidad Pública de Navarra (UPNA), IdiSNA. Irunlarrea, 3 31008*

9   *Pamplona, Spain; ² Proteored-ISCIII. Proteomics Unit, Navarrabiomed, Complejo*

10   *Hospitalario de Navarra (CHN), Universidad Pública de Navarra (UPNA), IdiSNA.*

11   *Irunlarrea, 3 31008 Pamplona, Spain; ³ Proteomics Platform, CIC bioGUNE,*

12   *CIBERehd, ProteoRed-ISCIII, Bizkaia Science and Technology Park, Derio, Spain;*

13   *⁴Institut de Neuropatologia, IDIBELL-Hospital Universitari de Bellvitge, Universitat de*

14   *Barcelona, L'Hospitalet de Llobregat, CIBERNED, Spain; ⁵ Centre for Brain Sciences,*

15   *Imperial College London, London, UK*

16

17   § These authors share senior authorship

18   To whom correspondence should be addressed: Proteomics Unit, Navarrabiomed

19   Biomedical Research Center Instituto de Investigación Sanitaria de Navarra (IdiSNA),

20   Pamplona, Spain. E-mail: esantamma@navarra.es (E. Santamaría)

21

22

23

24

25

26

27

28

29

Abstract

Olfactory dysfunction is one of the earliest features in Lewy-type alpha-synucleinopathies (LTS) such as Parkinson´s disease (PD). However, the underlying molecular mechanisms associated to smell impairment are poorly understood. Applying mass spectrometry-based quantitative proteomics in postmortem olfactory bulbs (OB) across limbic, early-neocortical, and neocortical LTS stages of parkinsonian subjects, a proteostasis impairment was observed, identifying 268 differentially expressed proteins between controls and PD phenotypes. In addition, network-driven proteomics revealed a modulation in ERK1/2, MKK3/6, and PDK1/PKC signalling axis. Moreover, a cross-disease study of selected olfactory molecules in sporadic Alzheimer's disease (AD) cases, revealed different protein derangements in the modulation of Secretagogin (SCGN), Calcyclin binding protein (CACYBP), and Glucosamine 6 phosphate isomerase 2 (GNPDA2) between PD and AD. An inverse correlation between GNPDA2 and α-synuclein protein levels was also reflected in PD cerebrospinal fluid (CSF). Interestingly, PD patients exhibited significantly lower serum GNPDA2 levels than controls (n=82/group). Our study provides important avenues for understanding the OB proteostasis imbalance in PD, deciphering mechanistic clues to the equivalent smell deficits observed in AD and PD pathologies.

Keywords: Parkinson's disease, Olfactory bulb, Proteomics, Systems Biology

49

50

51

52

53

54 **Abbreviations**

55 AD: Alzheimer´s disease

56 CACYBP: Calcyclin binding protein

57 CPNE6: Copine-6

58 DPP6: Dipeptidyl aminopeptidase-like protein 6

59 GNPDA2: Glucosamine 6 phosphate isomerase 2

60 LBD: Lewy body disease

61 LTS: Lewy-type alpha-synucleinopathy

62 OB: olfactory bulb

63 PD: Parkinson´s disease

64 RACK1: Receptor of activated protein C kinase 1

65 SCGN: secretagogin

66

67 **1. Introduction**

68 Olfactory dysfunction is present in up to 95% of PD patients (Attems et al., 2014; Doty,

69 2012b). In Lewy body diseases (LBDs), including PD, the olfactory deficit is an early

70 prodromal event being considered as a premotor sign of neurodegeneration (Baba et al.,

71 2012; Beach et al., 2009; Doty, 2008, 2012b). The initial induction of α-synuclein

72 misfolding and subsequent deposition, probably occurs in the olfactory bulb (OB)

73 and/or the enteric nervous system (Klingelhoefer and Reichmann, 2015; Rey et al.,

74 2016). Clinical features of olfactory dysfunction have been correlated with the presence

75 of Lewy-type alpha-synucleopathy (LTS) in different olfactory areas (Attems et al.,

76 2014; Beach et al., 2009; Saito et al., 2016; Ubeda-Banon et al., 2010a; Ubeda-Banon et

77 al., 2012; Ubeda-Banon et al., 2010b). Furthermore, microstructural white matter

78 reductions in the olfactory system, the reduction of the cholinergic centrifugal inputs to

79 the OB, and the increased number of the dopaminergic cells observed in the OB, have

80 also been suggested as potential origins of smell loss (Ibarretxe-Bilbao et al., 2010;

81 Mundinano et al., 2011; Mundinano et al., 2013).

82 PD and Dementia with Lewy bodies (DLB) are Lewy body diseases (LBD) because of

83 the presence of typical intracytoplasmic neuronal inclusions named Lewy bodies (LB)

84 together with Lewy neurites containing abnormal α-synuclein. Systematic study of

85 cases with LB pathology has prompted a staging classification of PD (and LBDs) from

86 the medulla oblongata and OB to the midbrain, diencephalic nuclei, and neocortex

87 (Braak et al., 2002; Braak et al., 2003; Braak et al., 2004). Stages 1, 2, 3 reflect,

88 respectively, LB pathology in the medulla oblongata, pons and midbrain; stage 4

89 includes, in addition, the basal prosencephalon and mesocortex; stage 5 extends to

90 sensory association areas of the neocortex and prefrontal neocortex; and stage 6

91 includes, in addition, lesions in first order sensory association areas of the neocortex and

92 pre-motor areas(Braak et al., 2002; Braak et al., 2003; Braak et al., 2004). Similar

93 categorization of LB pathology was used to classify DLB (McKeith et al., 2017;

94 McKeith et al., 2005; McKeith et al., 1996). The later classification covers three stages:

95 brain stem, limbic and neocortical. Atypical cases not following a clear gradient of LB

96 pathology from the lower brain stem and olfactory regions to the neocortex constitute

97 about ten percent of total LBDs (Braak et al., 2006; Jellinger, 2008, 2009). The most

98 frequent atypical LBD is the amygdala-predominant which was added as a peculiar

99 form to the former LBD-brain stem, LBD-limbic and LBD-neocortical classification

100 (Leverenz et al., 2008). All these classifications are based on the putative progression

101 with time of LB pathology in the brain from the medulla oblongata and OB to the

102 neocortex. Neuropathological studies have pointed out that the presence and severity of

103 α-synuclein pathology in the OB reflects the presence and severity of synucleinopathy

104 in other brain regions (Attems et al., 2014; Beach et al., 2009). Some studies have

105 demonstrated that the presence of LTS in the OB predicts with 90% sensitivity and

106 specificity the existence of neuropathologically confirmed PD (Beach et al., 2009).

107 Moreover, the sensitivity and specificity of clinical olfactory testing in differentiating

108 PD from non-PD ranges from 80% to 100% (Doty, 2012a). In addition, an OB atrophy

109 and a significant reduction in olfactory performance have been detected in PD respect to

110 control subjects (Brodoehl et al., 2012; Li et al., 2016). In view of these clinical and

111 neuropathological data, an in depth molecular characterization of the OB

112 neurodegeneration is necessary to reveal the missing links in the biochemical

113 understanding of the early smell impairment in PD.

114 In this work, we applied mass-spectrometry based quantitative proteomics as a

115 discovery platform to explore the magnitude and chronology of the OB proteome

116 modulation across limbic, early-neocortical, and neocortical LTS stages in PD cases,

117 also named LBD-limbic stage, LBD-early neocortical stage, and LBD neocortical stage.

118 First, we have used a novel technique, called MALDI-IMS, or MALDI - Imaging. The

119 use of MALDI-IMS offers the great advantage to investigate the physiopathological

120 changes taking place directly in tissue while retaining the histopathological context,

121 enabling the so-called "Molecular Histology" (Caprioli et al., 1997; Chaurand et al.,

122 2004). Second, we have applied a label-free shotgun proteomic approach getting more

123 than 250 differential expressed proteins between controls and PD-related phenotypes,

124 pinpointing specific pathways, protein interaction networks, and potential novel

125 therapeutic targets.

126   **2. Materials and methods**

127 *2.1 Materials* - The following reagents and materials were used: anti-GAPDH

128 (Calbiochem), anti-MKK3, anti-MKK6, anti-phospho MKK3 (Ser189)/MKK6

129 (Ser207), anti-p38 MAP kinase, anti-phospho p38 MAP kinase (Thr180/Tyr 182), anti-

130 p38 MAPK alpha, anti-p38 MAPK beta, anti-PDK1, anti-phospho PDK1 (S241), anti-

131 PKC-Pan, anti-phospho PKC-pan (T514), anti-pAkt (Ser473), anti-Akt, anti-pERK1/2

132 (Thr202/Tyr204), anti-ERK1/2 and anti-CACYBP (Cell Signaling), anti-CPNE6

133 (Thermo), anti-GNPDA2, anti-NEGR1, anti-RACK1, anti-SCGN (Abcam), anti-α-

134 synuclein (Santa Cruz Biotech), and anti-DPP6 (Sigma). Electrophoresis reagents were

135 purchased from Bio-rad and trypsin from Promega.

136 *2.2 Human samples* – According to the Spanish Law 14/2007 of Biomedical Research,

137 inform written consent forms were obtained for research purposes from relatives of

138 patients included in this study. The study was conducted in accordance with the

139 Declaration of Helsinki and all assessments, post-mortem evaluations, and procedures

140 were previously approved by the Clinical Ethics Committee of Navarra Health Service.

141 OB specimens (table 1), CSF samples (additional file 7) and associated clinical and

142 neuropathological data from PD subjects were supplied by the Parkinson's UK Brain

143 Bank, funded by Parkinson's UK, a charity registered in England and Wales (258197)

144 and in Scotland (SC037554), and the Neurological Tissue Bank from Navarrabiomed

145 (Pamplona, Spain). Neuropathological assessment was performed according to

146 standardized neuropathological scoring/grading systems (Alafuzoff et al., 2009).

147 Twenty-one PD cases were distributed into: LBD-limbic stage (LBDL) (n=7), LBD-

148 early neocortical stage (LBDE) (n=6), and LBD-neocortical stage (LBDN) (n=8). Eight

149 cases from elderly subjects with no history or histological findings of any neurological

150 disease were used as a control group. For validation and specificity analysis, OB

151 specimens and associated neuropathological data from AD subjects (n=14), were

152 supplied by the Neurological Tissue Bank of the Biobank from the Hospital Clinic-

153 Institut d'Investigacions Biomèdiques August Pi i Sunyer (IDIBAPS), and the

154   Neurological Tissue Bank of HUB-ICO-IDIBELL (Barcelona, Spain). All human brains

155   considered in this study (n=43) had a post-mortem interval (PMI) lower than 26 hours

156   (Table 1). Serum samples and data from patients included in the study were provided by

157   the Biobank of the University of Navarra and were processed following standard

158   operating procedures approved by the Ethical and Scientific Committees (Additional

159   file 1).

160   *2.3 MALDI imaging mass spectrometry (IMS)* - OBs from three different conditions

161   were washed with PBS and immediately frozen and stored at − 80 °C until analyzed in

162   order to preserve the native tissue morphology and minimize protein degradation.

163   Sample tissues were sectioned at 14 μm using a Leica RM2235 cryostat (Leica,

164   Wetzlar, DE) and thaw-mounted on ITO-coated glass slides (Bruker Daltonics, Bremen,

165   DE) for mass spectrometry (MS) analysis, following previously published protocols

166   (Lloro et al., 2017; Mourino-Alvarez et al., 2016).

167   *2.4 Sample preparation for shotgun proteomics* - OB specimens derived from control

168   and PD cases were homogenized in lysis buffer containing 7 M urea, 2 M thiourea, 4%

169   (w/v) CHAPS, 50 mM DTT. The homogenates were spinned down at 100.000 x g for 1

170   h at 15°C. Prior to proteomic analysis, protein extracts were precipitated with

171   methanol/choloroform, and pellets dissolved in 6M Urea, Tris 100mM pH 7.8. Protein

172   quantitation was performed with the Bradford assay kit (Bio-Rad).

173   *2.5 Label free LC-MS/MS* –Protein enzymatic cleavage (10ug) was carried out with

174   trypsin (Promega; 1:20, w/w) at 37°C for 16 h as previously described (Shevchenko et

175   al., 2006). Peptides mixtures were separated by reverse phase chromatography using an

176   Eksigent nanoLC ultra 2D pump fitted with a 75 μm ID column (Eksigent 0.075 x 250).

177   Samples were first loaded for desalting and concentration into a 0.5 cm length 100 μm

178   ID precolumn packed with the same chemistry as the separating column. Mobile phases

179 were 100% water 0.1% formic acid (FA) (buffer A) and 100% Acetonitrile 0.1% FA

180 (buffer B). Column gradient was developed in a 240 min two step gradient from 5% B

181 to 25% B in 210 min and 25%B to 40% B in 30 min. Eluting peptides were analyzed

182 using a 5600 Triple-TOF system, as previously described (Lachen-Montes et al., 2017).

183 *2.6 Peptide Identification and Quantification* – MS/MS data acquisition, searching,

184 peptide quantitation, and statistical analysis were performed as previously described

185 (Lachen-Montes et al., 2017). MS raw data and search results files have been deposited

186 to the ProteomeXchange Consortium (http://proteomecentral.proteomexchange.org) via

187 the PRIDE partner repository (Vizcaino et al., 2014) with the dataset identifiers

188 PXD008036.

189 *2.7 Statistical analysis* - The statistical analysis used for the identification of

190 differentially expressed proteins was performed using the Progenesis software and R

191 scripts. Before applying any statistical test, data were submitted to several mathematical

192 algorithms to remove the background, to align and compensate the ''between-run

193 variation'', and to choose the same peaks in all samples in the peak picking phase.

194 Then, peptides were identified with the information obtained using Protein Pilot

195 software. Output files with the identified proteins were then managed with R scripts for

196 subsequent statistical analysis. One-way ANOVA test was applied to compare the

197 results between all groups and unpaired Student's t-test was used for direct comparisons

198 between two groups of samples. Statistical significance was set at $p<0.05$ in all cases

199 and 1% peptide FDR (False discovery rate) threshold was considered (calculated based

200 on the search results against a decoy database). Additionally, an absolute fold change

201 of <0.77 (down-regulation) or >1.3 (up-regulation) in linear scale was considered to be

202 significantly differentially expressed. Concerning the immunoassays, the comparison

203 made between the neuropathological groups and the neurological intact control group

204   was performed using the unpaired T test for independent samples. A p value <0.05 was

205   considered significant. Results are represented as mean ± SE and errors bars show the

206   standard error of the mean from the samples used in each group.

207   *2.8 Bioinformatics* –The proteomic information was analyzed using Reactome (Fabregat

208   et al., 2018) in order to detect and infer differentially activated/deactivated pathways as

209   a result of PD phenotypes. The identification of specifically dysregulated

210   regulatory/metabolic networks across PD stages was analysed through the use of

211   QIAGEN's Ingenuity® Pathway Analysis (IPA) (QIAGEN Redwood City,

212   www.qiagen.com/ingenuity).

213   *2.9 Immunoblotting analysis* - In the case of CSF samples, 100-150µl were precipitated

214   with four volumes of acetone o/n at -20ºC. Then, samples were centrifuged during 15

215   minutes at 14000rpm to obtain the protein pellet. Equal amounts of OB protein (10 µg)

216   or CSF protein (8 µg) were resolved in 4-15% TGX stain-Free gels (Bio-Rad). Western-

217   blot analysis were performed as previously described (Lachen-Montes et al., 2017).

218   After densitometric analyses (Image Lab Software Version 5.2; Bio-Rad), optical

219   density values were expressed as arbitrary units and normalized to GAPDH (tissue

220   analysis) or to total stain in each gel lane (CSF analysis) (Moritz, 2017).

221   *2.10 Enzyme-Linked Immunosorbent Assay*. Serum GNPDA2 concentrations were

222   measured using enzyme-linked immunosorbent assay (ELISA) kits according to the

223   manufacturer's instructions (MBS93411798; MyBiosource). The detection range was

224   0.62 ng/ml – 20 ng/ml. Data were analyzed using Graphpad Prism software. Mann–

225   Whitney U test was used for between-group comparisons. We considered p-value less

226   than 0.05 to be statistically significant.

227   **Results**

228 ***3.1 Proteostasis impairment in the OB across Lewy-type alpha-synucleinopathy (LTS)***

229 ***staging***

230 In this work, we combined two complementary mass spectrometry-based proteomic

231 approaches such as MALDI-IMS and label-free quantitative proteomics to probe

232 additional molecular disturbances in post-mortem OBs dissected from clinically

233 confirmed PD cases respect to neurologically intact controls. First, MALDI-IMS was

234 applied for the first time in OB region to visualize in situ additional molecular

235 disturbances between control and LB neuropathological stages (Figure 1). Several

236 masses with differential spatial distribution between control and LB stages have been

237 found with ROC (Receiving Operating Characteristic) curves with statistical

238 significance (Area Under the Curve (AUC) >0.8). To determine and characterize the

239 progression and complexity of LTS-associated changes in this olfactory structure, the

240 OB site-specific proteomic signature was monitored across LTS staging using a

241 complementary label-free MS-based approach. Among 1629 quantified proteins across

242 all experimental groups, 268 proteins tend to be differentially expressed between

243 controls and PD phenotypes (Fig.2A and additional file 2). A progressive increment in

244 OB monomeric α-synuclein protein levels was also evidenced across LTS stages by

245 Western-blot (Fig.2B). Our analysis revealed that 148, 139, and 197 OB proteins are

246 differentially expressed in LBDL, LBDE, and LBDN stages, respectively. The

247 distribution between up-regulated and down-regulated proteins was very similar across

248 LTS grading (35-40% down-regulated, and 60-65% up-regulated proteins) (Fig. 2C).

249 Interestingly, 65 OB proteins overlapped between all stages (Fig. 2D), suggesting a

250 potential role during LTS progression in PD subjects. Most of these proteins mainly

251 clustered in specific biological process like transport and RNA processing with specific

252 molecular functions such as nucleotide binding and hydrolase activities (Additional file

253 3).

3.2 Olfactory dysregulated pathways across LTS grading

255 To extract biological knowledge, the differential OB proteome detected in each LTS

256 stage, was functionally categorized (Additional file 4). Immune system, metabolism of

257 lipids, aminoacids, and carbohydrates, signaling by growth factors and specific survival

258 pathways, together with vesicle-mediated transport and axon guidance were the

259 common over-represented dysregulated processes across LTS grading (Additional file

260 5A). To gain a more detailed description of the molecular mechanisms involved in the

261 OB during LB pathology, subsequent analyses were performed to explore the

262 differential olfactory proteome distributions across specific neuronal functionalities. As

263 shown in additional file 5B, our results point out a deregulation of specific protein

264 clusters related to cell death, basal ganglia dysfunction, and movement disorders.

265 Specifically, proteins involved in dyskinesia and tremor were exclusively mapped in

266 LBDN stage (Additional file 6). To characterize, in detail, the potential dysregulation of

267 LTS-related protein interactomes in the OB during the neurodegenerative process, we

268 have performed proteome-scale interaction networks merging the olfactory proteins that

269 tend to be deregulated in each LTS stage. Using IPA software, protein interactome maps

270 has been constructed for each LTS stage (Figure 3). In LBDL stage, the functional

271 interaction network indicated an alteration in HNRNP complexes (HNRNPA2B1,

272 HNRNPM, HNRNPC, HNRNPH3, HNRNPR), RNA binding proteins (ILF2, MATR3,

273 DDX6), as well as transcriptional and translational repressors (XRCC5, RACK1,

274 RUVBL1) suggesting an impairment in RNA stability and pre-mRNA splicing

275 processes (Figure 3A). In LBDE stage, the proteome-scale interaction network reflected

276 an alteration in multiple interactors of nucleophosmin (NPM1), reinforcing the

277   transcriptional derangements that occur at the level of the OB (Figure 3B). The

278   functional clustering also suggested an imbalance in signaling molecules involved in

279   cell survival and differentiation such as CSNK2B, LIMS1, and PP2A (Figure 3B). In

280   LBDN stage, functional interactors of specific survival routes were compromised,

281   suggesting an imbalance in the survival potential of olfactory neurons (Figure 3C).

282   *3.3 Network-driven proteomics reveals olfactory derangements in survival pathways*

283   *in Parkinson´s disease*

284   Signaling modulators like ERK, Akt, CaMKII, PKC and p38 MAPK appeared as

285   principal nodes in protein interactome maps (figure 3). Subsequent experiments were

286   performed to monitor the activation state of this kinase panel across LTS staging.

287   Respect to MAPK pathway, a significant increment in the steady-state levels of MEK

288   was observed in LBDN stage. On the contrary, a progressive down-regulation of ERK

289   levels was evidenced across LTS staging (figure 4A). Phosphoinositide-dependent

290   protein kinase 1 (PDK1) activity depends on the autophosphorylation on Ser241,

291   activating PKC signal transduction (Mora et al., 2004). Despite the up-regulation in

292   total PDK1 levels observed in LBDL stage, PDK1 was inactivated across LBDE and

293   LBDN stages (figure 4B). Moreover, PDK1 inactivation was accompanied by a

294   decrease in the activation status of PKC isoforms in LBDE stage, as revealed by

295   Western-blot using a specific pan-antibody against phosphorylated PKC isoforms

296   (Figure 4B). MKK3 and MKK6 are dual-specificity protein kinases that activate p38

297   MAPK (Derijard et al., 1995). We evaluated the activation state of olfactory MKK3-

298   6/p38 MAPK axis across LTS staging. As shown in figure 4C, MKK3/6 were

299   significantly inactivated across all stages, mainly due to a drop in total MKK6 levels.

300   On the other hand, no significant changes were observed in the activation state of p38

301   MAPK, detecting an over-expression of p38-alpha and -beta subunits in LBDL stage,

302 and a specific increment of p38-alpha protein in LBDN stage (Figure 4C). These data

303 suggest the existence of upstream disruption of olfactory MAPK, PDK1/PKC, and

304 MKK3-6/p38 MAPK axis among neuropathological stages. On the other hand, a

305 slightly increment in the activation state of Akt and CaMKII was observed in LBDL

306 stage, although these changes were not statistically significant (Figure 4D).

307 *3.4 Searching common pathological olfactory substrates in AD and PD phenotypes*

308 It has been recently proposed the potential existence of common olfactory pathological

309 substrates in AD and PD, mainly due to the equivalent severe olfactory deficits present

310 at earliest stages of both neurological syndromes (Doty, 2012b, 2017). With the aim to

311 identify common olfactory protein intermediates deregulated in both neurodegenerative

312 backgrounds, a cross-disease study of selected olfactory molecules was performed in

313 sporadic AD cases. For that, OB samples derived from low (Braak I-II), intermediate

314 (Braak III-IV), and high AD (Braak V-VI) were included in the cross-disease study

315 (Table 1). The selection of assessing the protein panel for verification was based

316 primarily on: i) differential expression across LTS stages and novelty in human PD

317 pathophysiology (SCGN, CACYBP, GNPDA2, RACK1) and ii) differential expression

318 in the OB from different neurological disorders (CPNE6, and DPP6) (Zelaya et al.,

319 2015). Our group has previously identified CPNE6 (Copine-6) and DPP6 (Dipeptidyl

320 aminopeptidase-like protein 6) as olfactory protein mediators deregulated in specific

321 neurological syndromes (Zelaya et al., 2015). As shown in figure 4E, olfactory CPNE6

322 and DPP6 protein levels were significantly increased in LBDL and LBDN stages.

323 SCGN (Secretagogin) is a calcium binding protein considered marker of periglomerular

324 and deep-layer olfactory interneurons (Attems et al., 2012). CACYBP (Calcyclin

325 binding protein) is involved in cytoskeletal dynamics and in the regulation of

326 transcriptional responses in neurons (Filipek et al., 2008; Kilanczyk et al., 2015).

327   GNPDA2 (Glucosamine 6 phosphate isomerase 2) participates in the glucose

328   metabolism, converting D-glucosamine-6-phosphate into D-fructose-6-phosphate and

329   ammonium (Arreola et al., 2003). RACK1 (Receptor of activated protein C kinase 1)

330   protects neurons from oxidative-stress-induced apoptosis (Ma et al., 2014). First, and

331   with the aim to complement and partially validate our proteomic workflow, the steady-

332   state levels of our protein panel were checked across LTS staging by Western blotting.

333   In accordance with our proteomic findings, the immunoblots confirmed the olfactory

334   over-expression of SCGN, GNPDA2, and RACK1 across LTS stages (Figure 4F). In

335   addition, a significant down-regulation of CACYBP was observed in LBDE, and LBDN

336   stages (Figure 4F). The monitorization of the expression of our protein panel in the OB

337   from AD cases (Figure 5A) revealed that: i) SCGN protein levels were down-regulated

338   in the OB derived from high AD cases, ii) CACYBP was specifically over-expressed in

339   low AD cases, iii) a significant increment in OB GNPDA2 protein levels across low and

340   intermediate AD, iv) no significant changes in OB RACK1 were observed across AD

341   staging. This cross-disease analysis revealed the existence of common protein

342   intermediates that are differentially deregulated during PD and AD progression at the

343   level of the OB.

344   *3.5 GNPDA2 protein biofluid profile differs between controls and PD subjects*

345   We further examined whether our protein panel could be detected in the CSF of PD

346   subjects and ultimately serves as potential novel PD biomarkers. Interestingly,

347   GNPDA2 was previously characterized by mass-spectrometry in CSF (Guldbrandsen et

348   al., 2014). Subsequent experiments were performed to check the GNPDA2 expression

349   in the CSF of PD patients (n=16) and healthy control subjects (n=9) (Additional file 7)

350   by Western-blot analysis. As shown in figure 5B, GNPDA2 protein levels were

351   significantly increased in CSF from PD patients respect to controls, showing an inverse

352 correlation between GNPDA2 and α -synuclein protein levels detected in CSF.

353 However, serum GNPDA2 levels were decreased in PD population (Figure 6)

354 (Additional file 1), suggesting that the GNPDA2 profiles observed in both biofluids

355 may be a consequence of the damaged blood-brain barrier (BBB) previously observed

356 in PD (Sweeney et al., 2018).

357 **4. Discussion**

358 In view of the general recognition that olfactory dysfunction is an early feature of PD,

359 we consider that the elucidation of the progressive proteome-wide alterations that

360 occurs in the OB, might provide novel candidate proteins for a druggability assessment

361 in PD. Neuroproteomics has been successfully applied to discover novel protein

362 mediators associated with PD pathogenesis, diagnosis and evolution (Jin et al., 2006;

363 Lehnert et al., 2012; Licker et al., 2012; Licker et al., 2014; Liu et al., 2015). To our

364 knowledge, this is the first study to characterize potential PD-associated molecular

365 changes in the human OB combining imaging mass-spectrometry and quantitative

366 proteomics. In a first approach, using MALDI-IMS as a molecular histology technique,

367 we have observed that there are obvious molecular changes between control and LB

368 stages, at protein level, with several distinctive masses (ROC curves with AUC values

369 >0.8) adopting marked positional domains in LB stages. Our data suggest that MALDI-

370 IMS is a suitable approach that complements current neuropathological classifications.

371 Some of the differential expressed OB proteins detected across LTS stages have been

372 proposed as α-synuclein interactors or protein components of Lewy body inclusions

373 (Betzer et al., 2015; Leverenz et al., 2007): IGSF8 (in LBDL stage), GNAO1, OMG,

374 ARPC5, and NIPSNAP1 (in LBDE stage), HSD17B10, ATP6V1D, PGRMC1,

375 ACADS, and TUBB2 (in LBDN stage), VPS53 (common to LBDL and LBDE stages),

376 ATP1A2, EHD1, EEF1A2, and BANF1 (common to LBDE and LBDN stages), and

377 TUBB4A, TPPP, and TUBA4A (common to all stages). To establish a functional

378 relationship between the OB and other PD-affected regions at proteome level, a

379 traceability analysis was performed comparing the differential OB protein set with

380 respect to deregulated proteins previously detected in functionally related structures

381 such as SN, striatum, and cortex derived from PD subjects (Licker et al., 2014; Riley et

382 al., 2014). In accordance with down-regulated OB proteome, the expression of five

383 nigral proteins, three cortical proteins, and striatal protein OMG were also down-

384 modulated in PD. In contrast, nigral protein MYO6, fourteen striatal proteins, and

385 eighteen cortical proteins present an opposite expression pattern (up-regulation) in PD

386 subjects (Additional file 8). With respect to the up-regulated OB proteome, four nigral

387 proteins, twenty striatal proteins, and seventeen cortical proteins were also up-regulated

388 in PD phenotypes (Additional file 8). This information suggests that the coordinated

389 deregulation of specific protein modules shared among brain areas might explain, in

390 part,   the   existence   of   conserved   transcriptional   programs   that   may   be

391 activated/deactivated across structures during PD pathogenesis.

392 The aberrant regulation of a subset of kinases may represent the triggering events

393 leading to the spread of an abnormal signaling in PD (Wang et al., 2012). In this

394 context, cell survival mechanisms have been proposed as targets for neuroprotective

395 strategies in delay onset, or slow progression of PD (Goswami et al., 2017). Analyzing

396 the signaling interactions predicted by our network-system biology approach, we

397 determine potential upstream regulators highly interconnected with deregulated

398 olfactory proteins. An increment in phospho-ERK levels has been previously reported

399 in midbrain dopaminergic neurons in PD brains (Zhu et al., 2003; Zhu et al., 2002).

400 However, in leukocytes, ERK1/2 activity does not significantly differ between controls

401 and PD subjects (White et al., 2007). In our case, the activation of the pro-survival

402 factor ERK1/2 tends to be compromised across LTS stages. Interestingly, a

403 hyperactivation of upstream MEK1/2 and ERK1/2 was evidenced in the OB derived

404 from AD subjects (Lachen-Montes et al., 2016), suggesting that MAPK signalling

405 clearly differs between PD and AD phenotypes at olfactory level. It has been shown

406 that p38 MAPK is activated by α-synuclein (Rannikko et al., 2015), being localized in

407 neurons of PD brain stem bearing LBs or α-synuclein deposits (Ferrer et al., 2001). An

408 early inactivation of MKK3/6-p38 MAPK axis has been observed in initial AD stages at

409 OB level, recovering normal levels in intermediate and advanced AD stages (Lachen-

410 Montes et al., 2017). However, a distinct profile was observed in PD phenotypes. The

411 inactivation of MKK3/6 across LTS stages suggests the involvement of other kinase-

412 based route in the apparent maintenance of olfactory p38 MAPK activity in the OB

413 from PD. To our knowledge, our data represent the first molecular link between PDK1

414 dysregulation and PD. An impairment of olfactory PDK1/PKC signaling axis was

415 observed in LBDL and LBDE stages. Interestingly, and in line with these findings, this

416 pathway is also modified in the OB of AD subjects (Lachen-Montes et al., 2017). As α-

417 synuclein specifically downregulates PKCδ isoform in dopaminergic cells (Jin et al.,

418 2011), further work will be necessary to clarify the specific role of each PKC isoform in

419 olfactory neurons during PD progression.

420 Although the activation state of specific olfactory survival pathways differs between PD

421 and AD, this study has allowed the identification of a subset of common protein

422 intermediates in the OB from PD and AD subjects respect to non-demented controls,

423 suggesting that these shared proteins might participate as common pathological

424 substrates during the olfactory neurodegenerative process in both neurological disorders

425 (Doty, 2012b, 2017). However, it is important to note that 14 out of 21 (67%) PD

426 subjects included in our study, present concomitant AD-type Tau pathology (Braak

427 stage I-II) (data not shown). Said that, we cannot exclude the possibility that the shared

428 differential OB proteome observed between AD and PD may be due to the AD

429 concomitant pathology present in PD subjects. In the present study, novel common

430 mediators have emerged but with different expression profiling between PD and AD

431 phenotypes, emphasizing the importance of neuropathological stage-dependent analysis

432 in the search of potential olfactory therapeutic targets. CPN6, and DPP6 tend to be up-

433 regulated in the OB from PD subjects, indicating specific differences in spine plasticity

434 and synaptic function (Lin et al., 2013; Reinhard et al., 2016) respect to AD (Zelaya et

435 al., 2015). Moreover, the different expression profile observed between AD and LTS

436 stages for SCGN, CACYBP, and RACK1 proteins also points out subtle differences in

437 calcium fluxes, cytoskeletal dynamics, and oxidative response in the OB from AD and

438 PD subjects. Interestingly, the metabolic enzyme GNPDA2 was over-expressed in most

439 PD and AD cases (see also additional file 9B), showing an inverse correlation between

440 GNPDA2 and α-synuclein protein levels in the CSF from PD subjects. However, serum

441 GNPDA2 levels were significantly decreased in PD population. The different protein

442 profile across fluids has been also observed for other proteins in the context of PD such

443 as Complement C4, serotransferrin, apolipoprotein AI, haptoglobin, zinc-alpha-2-

444 glycoprotein, Apolipoprotein E, beta-2-glycoprotein, ceruloplasmin, complement C3

445 and serum albumin (Halbgebauer et al., 2016). The lack of standardization between

446 laboratories in CSF collection and preparation procedures may be a reason for this type

447 of observation. However, from a biological point of view, these molecular events may

448 be due to the damage of the blood-brain barrier (BBB) observed in PD subjects

449 (Alexander et al., 1994; Kortekaas et al., 2005; Sweeney et al., 2018). Checking the

450 Human Protein Atlas (Uhlen et al., 2010)(www.proteinatlas.org), GNPDA2 is highly

451 expressed   by   the   brain   (https://www.proteinatlas.org/ENSG00000163281-

452 GNPDA2/tissue), so additional experiments are needed to explain the GNPDA2 efflux,

453 rates, and transportation (both the brain-to-blood and the blood-to-brain directions) in

454 the PD pathophysiology. Being aware of the small number of cases assessed in this

455 study, the novel relation of secreted GNPDA2, and α-synuclein should be further

456 evaluated in combination with other biochemical markers in order to improve the

457 current diagnostic assays (Eusebi et al., 2017; Forland et al., 2018).

458 **3. Conclusion**

459 Overall, the current study provides new insights regarding the molecular mechanisms

460 governing the olfactory dysfunction occurring during PD progression. Besides the

461 pathological depositions of α-synuclein occurring at the level of the OB, we have

462 demonstrated a clear disarrangement in the olfactory proteostasis, affecting cell survival

463 routes and showing potential common pathological substrates between PD and AD.

464 Moreover, the application of high-throughput proteomic approaches again proves to be

465 a useful tool to decipher the proteome expression profiles in olfactory structures and

466 more importantly, to define potential fluid biomarkers for the diagnosis of

467 neurodegenerative processes.

468 **Declarations**

469 **Ethics approval and consent to participate:** According to the Spanish Law 14/2007

470 of Biomedical Research, inform written consent forms were obtained for research

471 purposes from relatives of patients included in this study. The study was conducted in

472 accordance with the Declaration of Helsinki and all assessments, post-mortem

473 evaluations, and procedures were previously approved by the Clinical Ethics Committee

474 of Navarra Health Service.

475 **Consent for publication:** Not applicable

476

477 **Availability of data and materials:** MS raw data and search results files have been

478 deposited to the ProteomeXchange Consortium

479 (http://proteomecentral.proteomexchange.org) via the PRIDE partner repository with

480 the dataset identifiers PXD008036. (For reviewers: username:

481 reviewer45850@ebi.ac.uk; password: hBK0q6GD)

482 **Competing interests:** The authors declare that they have no competing interests.

483 **Funding:** This work was funded by grants from the Spanish Ministry of Economy and

484 Competitiveness (MINECO) (Ref. SAF2014-59340-R), Department of Economic

485 Development from Government of Navarra (Ref. PC023-PC024, PC025, PC081-82 and

486 PI059) and Obra Social la Caixa to ES. AGM was supported by PEJ-2014-A-61949

487 (MINECO). MLM is supported by a predoctoral fellowship from the Public University

488 of Navarra (UPNA).

489 **Author contributions:** JFI and ES designed and supervised the complete study. MLM,

490 and AGM performed proteomic experiments, bioinformatics analysis, protein validation

491 and signaling pathway characterizations. IL, and FE performed MALDI-IMS

492 experiments. IF, and DG performed neuropathological classifications. JFI and ES

493 performed mass spectrometry analysis and data interpretation. ES wrote the paper. All

494 authors reviewed the manuscript.

495 **Acknowledgements**

496 We are very grateful to the patients that generously donor the brain tissue, or fluid

497 samples for research purposes. We thank the collaboration of Parkinson's UK Brain

498 Bank funded by Parkinson's UK, a charity registered in England and Wales (258197)

499 and in Scotland (SC037554), the Neurological Tissue Bank of the Biobank from the

500 Hospital Clinic-Institut d'Investigacions Biomédiques August Pi i Sunyer (IDIBAPS,

501 Barcelona), the Neurological Tissue Bank of HUB-ICO-IDIBELL (Barcelona, Spain),

512 **Appendix A.** Supplementary data

513 **References**

522 Alafuzoff, I., Ince, P.G., Arzberger, T., Al-Sarraj, S., Bell, J., Bodi, I., Bogdanovic, N.,
523 Bugiani, O., Ferrer, I., Gelpi, E., Gentleman, S., Giaccone, G., Ironside, J.W.,
524 Kavantzas, N., King, A., Korkolopoulou, P., Kovacs, G.G., Meyronet, D., Monoranu,
525 C., Parchi, P., Parkkinen, L., Patsouris, E., Roggendorf, W., Rozemuller, A.,
526 Stadelmann-Nessler, C., Streichenberger, N., Thal, D.R., Kretzschmar, H., 2009.
527 Staging/typing of Lewy body related alpha-synuclein pathology: a study of the
528 BrainNet Europe Consortium. Acta Neuropathol 117(6), 635-652.
529 Alexander, G.M., Schwartzman, R.J., Grothusen, J.R., Gordon, S.W., 1994. Effect of
530 plasma levels of large neutral amino acids and degree of parkinsonism on the blood-to-
531 brain transport of levodopa in naive and MPTP parkinsonian monkeys. Neurology
532 44(8), 1491-1499.
533 Arreola, R., Valderrama, B., Morante, M.L., Horjales, E., 2003. Two mammalian
534 glucosamine-6-phosphate deaminases: a structural and genetic study. FEBS Lett 551(1-
535 3), 63-70.
536 Attems, J., Alpar, A., Spence, L., McParland, S., Heikenwalder, M., Uhlen, M., Tanila,
537 H., Hokfelt, T.G., Harkany, T., 2012. Clusters of secretagogin-expressing neurons in the
538 aged human olfactory tract lack terminal differentiation. Proc Natl Acad Sci U S A
539 109(16), 6259-6264.
540 Attems, J., Walker, L., Jellinger, K.A., 2014. Olfactory bulb involvement in
541 neurodegenerative diseases. Acta Neuropathol 127(4), 459-475.
542 Baba, T., Kikuchi, A., Hirayama, K., Nishio, Y., Hosokai, Y., Kanno, S., Hasegawa, T.,
543 Sugeno, N., Konno, M., Suzuki, K., Takahashi, S., Fukuda, H., Aoki, M., Itoyama, Y.,
544 Mori, E., Takeda, A., 2012. Severe olfactory dysfunction is a prodromal symptom of
545 dementia associated with Parkinson's disease: a 3 year longitudinal study. Brain 135(Pt
546 1), 161-169.

547 Beach, T.G., White, C.L., 3rd, Hladik, C.L., Sabbagh, M.N., Connor, D.J., Shill, H.A.,
548 Sue, L.I., Sasse, J., Bachalakuri, J., Henry-Watson, J., Akiyama, H., Adler, C.H., 2009.
549 Olfactory bulb alpha-synucleinopathy has high specificity and sensitivity for Lewy
550 body disorders. Acta Neuropathol 117(2), 169-174.
551 Betzer, C., Movius, A.J., Shi, M., Gai, W.P., Zhang, J., Jensen, P.H., 2015.
552 Identification of synaptosomal proteins binding to monomeric and oligomeric alpha-
553 synuclein. PLoS One 10(2), e0116473.
554 Braak, H., Del Tredici, K., Bratzke, H., Hamm-Clement, J., Sandmann-Keil, D., Rub,
555 U., 2002. Staging of the intracerebral inclusion body pathology associated with
556 idiopathic Parkinson's disease (preclinical and clinical stages). J Neurol 249 Suppl 3,
557 III/1-5.
558 Braak, H., Del Tredici, K., Rub, U., de Vos, R.A., Jansen Steur, E.N., Braak, E., 2003.
559 Staging of brain pathology related to sporadic Parkinson's disease. Neurobiol Aging
560 24(2), 197-211.
561 Braak, H., Ghebremedhin, E., Rub, U., Bratzke, H., Del Tredici, K., 2004. Stages in the
562 development of Parkinson's disease-related pathology. Cell Tissue Res 318(1), 121-134.
563 Braak, H., Muller, C.M., Rub, U., Ackermann, H., Bratzke, H., de Vos, R.A., Del
564 Tredici, K., 2006. Pathology associated with sporadic Parkinson's disease--where does it
565 end? J Neural Transm Suppl(70), 89-97.
566 Brodoehl, S., Klingner, C., Volk, G.F., Bitter, T., Witte, O.W., Redecker, C., 2012.
567 Decreased olfactory bulb volume in idiopathic Parkinson's disease detected by 3.0-tesla
568 magnetic resonance imaging. Mov Disord 27(8), 1019-1025.
569 Caprioli, R.M., Farmer, T.B., Gile, J., 1997. Molecular imaging of biological samples:
570 localization of peptides and proteins using MALDI-TOF MS. Anal Chem 69(23), 4751-
571 4760.
572 Chaurand, P., Schwartz, S.A., Billheimer, D., Xu, B.J., Crecelius, A., Caprioli, R.M.,
573 2004. Integrating histology and imaging mass spectrometry. Anal Chem 76(4), 1145-
574 1155.
575 Derijard, B., Raingeaud, J., Barrett, T., Wu, I.H., Han, J., Ulevitch, R.J., Davis, R.J.,
576 1995. Independent human MAP-kinase signal transduction pathways defined by MEK
577 and MKK isoforms. Science 267(5198), 682-685.
578 Doty, R.L., 2008. The olfactory vector hypothesis of neurodegenerative disease: is it
579 viable? Ann Neurol 63(1), 7-15.
580 Doty, R.L., 2012a. Olfaction in Parkinson's disease and related disorders. Neurobiol Dis
581 46(3), 527-552.
582 Doty, R.L., 2012b. Olfactory dysfunction in Parkinson disease. Nat Rev Neurol 8(6),
583 329-339.
584 Doty, R.L., 2017. Olfactory dysfunction in neurodegenerative diseases: is there a
585 common pathological substrate? Lancet Neurol 16(6), 478-488.
586 Eusebi, P., Giannandrea, D., Biscetti, L., Abraha, I., Chiasserini, D., Orso, M.,
587 Calabresi, P., Parnetti, L., 2017. Diagnostic utility of cerebrospinal fluid alpha-
588 synuclein in Parkinson's disease: A systematic review and meta-analysis. Mov Disord
589 32(10), 1389-1400.
590 Fabregat, A., Jupe, S., Matthews, L., Sidiropoulos, K., Gillespie, M., Garapati, P., Haw,
591 R., Jassal, B., Korninger, F., May, B., Milacic, M., Roca, C.D., Rothfels, K., Sevilla, C.,
592 Shamovsky, V., Shorser, S., Varusai, T., Viteri, G., Weiser, J., Wu, G., Stein, L.,
593 Hermjakob, H., D'Eustachio, P., 2018. The Reactome Pathway Knowledgebase. Nucleic
594 Acids Res 46(D1), D649-D655.
595 Ferrer, I., Blanco, R., Carmona, M., Puig, B., Barrachina, M., Gomez, C., Ambrosio, S.,
596 2001. Active, phosphorylation-dependent mitogen-activated protein kinase

597 (MAPK/ERK), stress-activated protein kinase/c-Jun N-terminal kinase (SAPK/JNK),
598 and p38 kinase expression in Parkinson's disease and Dementia with Lewy bodies. J
599 Neural Transm (Vienna) 108(12), 1383-1396.
600 Filipek, A., Schneider, G., Mietelska, A., Figiel, I., Niewiadomska, G., 2008. Age-
601 dependent changes in neuronal distribution of CacyBP/SIP: comparison to tubulin and
602 the tau protein. J Neural Transm (Vienna) 115(9), 1257-1264.
603 Forland, M.G., Ohrfelt, A., Dalen, I., Tysnes, O.B., Blennow, K., Zetterberg, H.,
604 Pedersen, K.F., Alves, G., Lange, J., 2018. Evolution of cerebrospinal fluid total alpha-
605 synuclein in Parkinson's disease. Parkinsonism Relat Disord 49, 4-8.
606 Goswami, P., Joshi, N., Singh, S., 2017. Neurodegenerative signaling factors and
607 mechanisms in Parkinson's pathology. Toxicol In Vitro 43, 104-112.
608 Guldbrandsen, A., Vethe, H., Farag, Y., Oveland, E., Garberg, H., Berle, M., Myhr,
609 K.M., Opsahl, J.A., Barsnes, H., Berven, F.S., 2014. In-depth characterization of the
610 cerebrospinal fluid (CSF) proteome displayed through the CSF proteome resource
611 (CSF-PR). Mol Cell Proteomics 13(11), 3152-3163.
612 Halbgebauer, S., Ockl, P., Wirth, K., Steinacker, P., Otto, M., 2016. Protein biomarkers
613 in Parkinson's disease: Focus on cerebrospinal fluid markers and synaptic proteins. Mov
614 Disord 31(6), 848-860.
615 Ibarretxe-Bilbao, N., Junque, C., Marti, M.J., Valldeoriola, F., Vendrell, P., Bargallo,
616 N., Zarei, M., Tolosa, E., 2010. Olfactory impairment in Parkinson's disease and white
617 matter abnormalities in central olfactory areas: A voxel-based diffusion tensor imaging
618 study. Mov Disord 25(12), 1888-1894.
619 Jellinger, K.A., 2008. A critical reappraisal of current staging of Lewy-related
620 pathology in human brain. Acta Neuropathol 116(1), 1-16.
621 Jellinger, K.A., 2009. A critical evaluation of current staging of alpha-synuclein
622 pathology in Lewy body disorders. Biochim Biophys Acta 1792(7), 730-740.
623 Jin, H., Kanthasamy, A., Ghosh, A., Yang, Y., Anantharam, V., Kanthasamy, A.G.,
624 2011. alpha-Synuclein negatively regulates protein kinase Cdelta expression to suppress
625 apoptosis in dopaminergic neurons by reducing p300 histone acetyltransferase activity.
626 J Neurosci 31(6), 2035-2051.
627 Jin, J., Hulette, C., Wang, Y., Zhang, T., Pan, C., Wadhwa, R., Zhang, J., 2006.
628 Proteomic identification of a stress protein, mortalin/mthsp70/GRP75: relevance to
629 Parkinson disease. Mol Cell Proteomics 5(7), 1193-1204.
630 Kilanczyk, E., Filipek, A., Hetman, M., 2015. Calcyclin-binding protein/Siah-1-
631 interacting protein as a regulator of transcriptional responses in brain cells. J Neurosci
632 Res 93(1), 75-81.
633 Klingelhoefer, L., Reichmann, H., 2015. Pathogenesis of Parkinson disease--the gut-
634 brain axis and environmental factors. Nat Rev Neurol 11(11), 625-636.
635 Kortekaas, R., Leenders, K.L., van Oostrom, J.C., Vaalburg, W., Bart, J., Willemsen,
636 A.T., Hendrikse, N.H., 2005. Blood-brain barrier dysfunction in parkinsonian midbrain
637 in vivo. Ann Neurol 57(2), 176-179.
638 Lachen-Montes, M., Gonzalez-Morales, A., de Morentin, X.M., Perez-Valderrama, E.,
639 Ausin, K., Zelaya, M.V., Serna, A., Aso, E., Ferrer, I., Fernandez-Irigoyen, J.,
640 Santamaria, E., 2016. An early dysregulation of FAK and MEK/ERK signaling
641 pathways precedes the beta-amyloid deposition in the olfactory bulb of APP/PS1 mouse
642 model of Alzheimer's disease. J Proteomics 148, 149-158.
643 Lachen-Montes, M., Gonzalez-Morales, A., Zelaya, M.V., Perez-Valderrama, E., Ausin,
644 K., Ferrer, I., Fernandez-Irigoyen, J., Santamaria, E., 2017. Olfactory bulb
645 neuroproteomics reveals a chronological perturbation of survival routes and a disruption
646 of prohibitin complex during Alzheimer's disease progression. Sci Rep 7(1), 9115.

647 Lehnert, S., Jesse, S., Rist, W., Steinacker, P., Soininen, H., Herukka, S.K., Tumani, H.,
648 Lenter, M., Oeckl, P., Ferger, B., Hengerer, B., Otto, M., 2012. iTRAQ and multiple
649 reaction monitoring as proteomic tools for biomarker search in cerebrospinal fluid of
650 patients with Parkinson's disease dementia. Exp Neurol 234(2), 499-505.
651 Leverenz, J.B., Hamilton, R., Tsuang, D.W., Schantz, A., Vavrek, D., Larson, E.B.,
652 Kukull, W.A., Lopez, O., Galasko, D., Masliah, E., Kaye, J., Woltjer, R., Clark, C.,
653 Trojanowski, J.Q., Montine, T.J., 2008. Empiric refinement of the pathologic
654 assessment of Lewy-related pathology in the dementia patient. Brain Pathol 18(2), 220-
655 224.
656 Leverenz, J.B., Umar, I., Wang, Q., Montine, T.J., McMillan, P.J., Tsuang, D.W., Jin,
657 J., Pan, C., Shin, J., Zhu, D., Zhang, J., 2007. Proteomic identification of novel proteins
658 in cortical lewy bodies. Brain Pathol 17(2), 139-145.
659 Li, J., Gu, C.Z., Su, J.B., Zhu, L.H., Zhou, Y., Huang, H.Y., Liu, C.F., 2016. Changes in
660 Olfactory Bulb Volume in Parkinson's Disease: A Systematic Review and Meta-
661 Analysis. PLoS One 11(2), e0149286.
662 Licker, V., Cote, M., Lobrinus, J.A., Rodrigo, N., Kovari, E., Hochstrasser, D.F., Turck,
663 N., Sanchez, J.C., Burkhard, P.R., 2012. Proteomic profiling of the substantia nigra
664 demonstrates CNDP2 overexpression in Parkinson's disease. J Proteomics 75(15), 4656-
665 4667.
666 Licker, V., Turck, N., Kovari, E., Burkhardt, K., Cote, M., Surini-Demiri, M., Lobrinus,
667 J.A., Sanchez, J.C., Burkhard, P.R., 2014. Proteomic analysis of human substantia nigra
668 identifies novel candidates involved in Parkinson's disease pathogenesis. Proteomics
669 14(6), 784-794.
670 Lin, L., Sun, W., Throesch, B., Kung, F., Decoster, J.T., Berner, C.J., Cheney, R.E.,
671 Rudy, B., Hoffman, D.A., 2013. DPP6 regulation of dendritic morphogenesis impacts
672 hippocampal synaptic development. Nat Commun 4, 2270.
673 Liu, Y., Zhou, Q., Tang, M., Fu, N., Shao, W., Zhang, S., Yin, Y., Zeng, R., Wang, X.,
674 Hu, G., Zhou, J., 2015. Upregulation of alphaB-crystallin expression in the substantia
675 nigra of patients with Parkinson's disease. Neurobiol Aging 36(4), 1686-1691.
676 Lloro, I., Fernandez-Irigoyen, J., Escobes, I., Azkargorta, M., Santamaria, E., Elortza,
677 F., 2017. Methods for human olfactory bulb tissue studies using peptide/protein
678 MALDI-TOF imaging mass spectrometry, in: Santamaria, E., Fernandez-Irigoyen, J.
679 (Eds.), Neuromethods. Humana Press, New York, NY, pp. 91-106.
680 Ma, J., Wu, R., Zhang, Q., Wu, J.B., Lou, J., Zheng, Z., Ding, J.Q., Yuan, Z., 2014. DJ-
681 1 interacts with RACK1 and protects neurons from oxidative-stress-induced apoptosis.
682 Biochem J 462(3), 489-497.
683 McKeith, I.G., Boeve, B.F., Dickson, D.W., Halliday, G., Taylor, J.P., Weintraub, D.,
684 Aarsland, D., Galvin, J., Attems, J., Ballard, C.G., Bayston, A., Beach, T.G., Blanc, F.,
685 Bohnen, N., Bonanni, L., Bras, J., Brundin, P., Burn, D., Chen-Plotkin, A., Duda, J.E.,
686 El-Agnaf, O., Feldman, H., Ferman, T.J., Ffytche, D., Fujishiro, H., Galasko, D.,
687 Goldman, J.G., Gomperts, S.N., Graff-Radford, N.R., Honig, L.S., Iranzo, A., Kantarci,
688 K., Kaufer, D., Kukull, W., Lee, V.M.Y., Leverenz, J.B., Lewis, S., Lippa, C., Lunde,
689 A., Masellis, M., Masliah, E., McLean, P., Mollenhauer, B., Montine, T.J., Moreno, E.,
690 Mori, E., Murray, M., O'Brien, J.T., Orimo, S., Postuma, R.B., Ramaswamy, S., Ross,
691 O.A., Salmon, D.P., Singleton, A., Taylor, A., Thomas, A., Tiraboschi, P., Toledo, J.B.,
692 Trojanowski, J.Q., Tsuang, D., Walker, Z., Yamada, M., Kosaka, K., 2017. Diagnosis
693 and management of dementia with Lewy bodies: Fourth consensus report of the DLB
694 Consortium. Neurology 89(1), 88-100.
695 McKeith, I.G., Dickson, D.W., Lowe, J., Emre, M., O'Brien, J.T., Feldman, H.,
696 Cummings, J., Duda, J.E., Lippa, C., Perry, E.K., Aarsland, D., Arai, H., Ballard, C.G.,

697 Boeve, B., Burn, D.J., Costa, D., Del Ser, T., Dubois, B., Galasko, D., Gauthier, S.,
698 Goetz, C.G., Gomez-Tortosa, E., Halliday, G., Hansen, L.A., Hardy, J., Iwatsubo, T.,
699 Kalaria, R.N., Kaufer, D., Kenny, R.A., Korczyn, A., Kosaka, K., Lee, V.M., Lees, A.,
700 Litvan, I., Londos, E., Lopez, O.L., Minoshima, S., Mizuno, Y., Molina, J.A.,
701 Mukaetova-Ladinska, E.B., Pasquier, F., Perry, R.H., Schulz, J.B., Trojanowski, J.Q.,
702 Yamada, M., 2005. Diagnosis and management of dementia with Lewy bodies: third
703 report of the DLB Consortium. Neurology 65(12), 1863-1872.
704 McKeith, I.G., Galasko, D., Kosaka, K., Perry, E.K., Dickson, D.W., Hansen, L.A.,
705 Salmon, D.P., Lowe, J., Mirra, S.S., Byrne, E.J., Lennox, G., Quinn, N.P., Edwardson,
706 J.A., Ince, P.G., Bergeron, C., Burns, A., Miller, B.L., Lovestone, S., Collerton, D.,
707 Jansen, E.N., Ballard, C., de Vos, R.A., Wilcock, G.K., Jellinger, K.A., Perry, R.H.,
708 1996. Consensus guidelines for the clinical and pathologic diagnosis of dementia with
709 Lewy bodies (DLB): report of the consortium on DLB international workshop.
710 Neurology 47(5), 1113-1124.
711 Mora, A., Komander, D., van Aalten, D.M., Alessi, D.R., 2004. PDK1, the master
712 regulator of AGC kinase signal transduction. Semin Cell Dev Biol 15(2), 161-170.
713 Moritz, C.P., 2017. Tubulin or Not Tubulin: Heading Toward Total Protein Staining as
714 Loading Control in Western Blots. Proteomics 17(20).
715 Mourino-Alvarez, L., Iloro, I., de la Cuesta, F., Azkargorta, M., Sastre-Oliva, T.,
716 Escobes, I., Lopez-Almodovar, L.F., Sanchez, P.L., Urreta, H., Fernandez-Aviles, F.,
717 Pinto, A., Padial, L.R., Akerstrom, F., Elortza, F., Barderas, M.G., 2016. MALDI-
718 Imaging Mass Spectrometry: a step forward in the anatomopathological characterization
719 of stenotic aortic valve tissue. Sci Rep 6, 27106.
720 Mundinano, I.C., Caballero, M.C., Ordonez, C., Hernandez, M., DiCaudo, C., Marcilla,
721 I., Erro, M.E., Tunon, M.T., Luquin, M.R., 2011. Increased dopaminergic cells and
722 protein aggregates in the olfactory bulb of patients with neurodegenerative disorders.
723 Acta Neuropathol 122(1), 61-74.
724 Mundinano, I.C., Hernandez, M., Dicaudo, C., Ordonez, C., Marcilla, I., Tunon, M.T.,
725 Luquin, M.R., 2013. Reduced cholinergic olfactory centrifugal inputs in patients with
726 neurodegenerative disorders and MPTP-treated monkeys. Acta Neuropathol 126(3),
727 411-425.
728 Rannikko, E.H., Weber, S.S., Kahle, P.J., 2015. Exogenous alpha-synuclein induces
729 toll-like receptor 4 dependent inflammatory responses in astrocytes. BMC Neurosci 16,
730 57.
731 Reinhard, J.R., Kriz, A., Galic, M., Angliker, N., Rajalu, M., Vogt, K.E., Ruegg, M.A.,
732 2016. The calcium sensor Copine-6 regulates spine structural plasticity and learning and
733 memory. Nat Commun 7, 11613.
734 Rey, N.L., Steiner, J.A., Maroof, N., Luk, K.C., Madaj, Z., Trojanowski, J.Q., Lee,
735 V.M., Brundin, P., 2016. Widespread transneuronal propagation of alpha-
736 synucleinopathy triggered in olfactory bulb mimics prodromal Parkinson's disease. J
737 Exp Med 213(9), 1759-1778.
738 Riley, B.E., Gardai, S.J., Emig-Agius, D., Bessarabova, M., Ivliev, A.E., Schule, B.,
739 Alexander, J., Wallace, W., Halliday, G.M., Langston, J.W., Braxton, S., Yednock, T.,
740 Shaler, T., Johnston, J.A., 2014. Systems-based analyses of brain regions functionally
741 impacted in Parkinson's disease reveals underlying causal mechanisms. PLoS One 9(8),
742 e102909.
743 Saito, Y., Shioya, A., Sano, T., Sumikura, H., Murata, M., Murayama, S., 2016. Lewy
744 body pathology involves the olfactory cells in Parkinson's disease and related disorders.
745 Mov Disord 31(1), 135-138.

746 Shevchenko, A., Tomas, H., Havlis, J., Olsen, J.V., Mann, M., 2006. In-gel digestion
747 for mass spectrometric characterization of proteins and proteomes. Nat Protoc 1(6),
748 2856-2860.
749 Sweeney, M.D., Sagare, A.P., Zlokovic, B.V., 2018. Blood-brain barrier breakdown in
750 Alzheimer disease and other neurodegenerative disorders. Nat Rev Neurol 14(3), 133-
751 150.
752 Ubeda-Banon, I., Saiz-Sanchez, D., de la Rosa-Prieto, C., Argandona-Palacios, L.,
753 Garcia-Munozguren, S., Martinez-Marcos, A., 2010a. alpha-Synucleinopathy in the
754 human olfactory system in Parkinson's disease: involvement of calcium-binding
755 protein- and substance P-positive cells. Acta Neuropathol 119(6), 723-735.
756 Ubeda-Banon, I., Saiz-Sanchez, D., de la Rosa-Prieto, C., Martinez-Marcos, A., 2012.
757 alpha-Synuclein in the olfactory system of a mouse model of Parkinson's disease:
758 correlation with olfactory projections. Brain Struct Funct 217(2), 447-458.
759 Ubeda-Banon, I., Saiz-Sanchez, D., de la Rosa-Prieto, C., Mohedano-Moriano, A.,
760 Fradejas, N., Calvo, S., Argandona-Palacios, L., Garcia-Munozguren, S., Martinez-
761 Marcos, A., 2010b. Staging of alpha-synuclein in the olfactory bulb in a model of
762 Parkinson's disease: cell types involved. Mov Disord 25(11), 1701-1707.
763 Uhlen, M., Oksvold, P., Fagerberg, L., Lundberg, E., Jonasson, K., Forsberg, M.,
764 Zwahlen, M., Kampf, C., Wester, K., Hober, S., Wernerus, H., Bjorling, L., Ponten, F.,
765 2010. Towards a knowledge-based Human Protein Atlas. Nat Biotechnol 28(12), 1248-
766 1250.
767 Vizcaino, J.A., Deutsch, E.W., Wang, R., Csordas, A., Reisinger, F., Rios, D., Dianes,
768 J.A., Sun, Z., Farrah, T., Bandeira, N., Binz, P.A., Xenarios, I., Eisenacher, M., Mayer,
769 G., Gatto, L., Campos, A., Chalkley, R.J., Kraus, H.J., Albar, J.P., Martinez-Bartolome,
770 S., Apweiler, R., Omenn, G.S., Martens, L., Jones, A.R., Hermjakob, H., 2014.
771 ProteomeXchange provides globally coordinated proteomics data submission and
772 dissemination. Nat Biotechnol 32(3), 223-226.
773 Wang, G., Pan, J., Chen, S.D., 2012. Kinases and kinase signaling pathways: potential
774 therapeutic targets in Parkinson's disease. Prog Neurobiol 98(2), 207-221.
775 White, L.R., Toft, M., Kvam, S.N., Farrer, M.J., Aasly, J.O., 2007. MAPK-pathway
776 activity, Lrrk2 G2019S, and Parkinson's disease. J Neurosci Res 85(6), 1288-1294.
777 Zelaya, M.V., Perez-Valderrama, E., de Morentin, X.M., Tunon, T., Ferrer, I., Luquin,
778 M.R., Fernandez-Irigoyen, J., Santamaria, E., 2015. Olfactory bulb proteome dynamics
779 during the progression of sporadic Alzheimer's disease: identification of common and
780 distinct olfactory targets across Alzheimer-related co-pathologies. Oncotarget 6(37),
781 39437-39456.
782 Zhu, J.H., Guo, F., Shelburne, J., Watkins, S., Chu, C.T., 2003. Localization of
783 phosphorylated ERK/MAP kinases to mitochondria and autophagosomes in Lewy body
784 diseases. Brain Pathol 13(4), 473-481.
785 Zhu, J.H., Kulich, S.M., Oury, T.D., Chu, C.T., 2002. Cytoplasmic aggregates of
786 phosphorylated extracellular signal-regulated protein kinases in Lewy body diseases.
787 Am J Pathol 161(6), 2087-2098.
788
789
790

791

792

793

794

795

796

797

Figure and table legends

Table 1. General characteristics of the subjects included in the study. LBDL: LBD-limbic stage; LBDE: LBD-early-neocortical stage; LBDN: LBD-neocortical stage.

Figure 1. MALDI imaging mass spectrometry of human OB. Mean spectra of the whole section of control OB (red) and each LTS stages (green), and the corresponding spatial distribution of the selected peaks. A) band at 1789 Th. B) band at 4205 Th. C) band at 2549 Th, and D) band at 15272 Th. This pattern can also be shown in the corresponding whisker-plots.

Figure 2. OB Differentially proteins across PD-related phenotypes. A) Volcano plots from the pair-wise comparisons: control vs LBDL stage (upper panel), LBDE stage (middle panel), and LBDN stage (lower panel). Differential proteins: P < 0.01 in green, and P < 0.05 in yellow. B) OB monomeric α-synuclein expression. C) Differential olfactory proteome distributions. D) Common and unique differential proteins between LTS stages.

Figure 3. Protein interactome maps for differentially expressed proteins in the OB during LTS progression. Visual representation of the relationships detected in LBDL (A), LBDE (B), and LBDN (C). Up-regulated proteins in red, and down-regulated proteins in green. Complete legend in http://ingenuity.force.com/ipa/articles/Feature_Description/Legend.

817   **Figure 4. Monitoring of OB survival routes and specific protein intermediates**

818   **across LTS grading.** Levels and phosphorylation of MAP kinases (A), PDK1/PKC (B),

819   MKK3-6/p38 MAPK (C), and AKT and CaMKII kinases (D) in the OB across PD

820   phenotypes. CPNE6 and DPP6 protein expression levels across LTS stages (E). Protein

821   variation in SCGN, CACYBP, GNPDA2, and RACK1 levels across PD phenotypes (F).

822   *P < 0.05 vs control group; ** P < 0.01 vs control group; *** P < 0.01 vs control group.

823   Statistical analysis between LTS stages is shown in additional file 9A.

824   **Figure 5. Monitoring of specific olfactory proteins during AD progression.**

825   **GNPDA2 and α-synuclein levels in the CSF of PD subjects.** A) Protein levels of

826   SCGN, CACYBP, GNPDA2, and RACK1 were monitored by Western-blotting across

827   AD stages. Statistical analysis between AD stages is shown in additional file 9B. B)

828   Inverse correlation between GNPDA2 and α-synuclein protein expression in CSF from

829   PD subjects. *P < 0.05 vs control group; ** P < 0.01 vs control group; *** P < 0.01 vs

830   control group.

831   **Figure 6. Serum GNPDA2 levels in PD population.** GNPDA2 levels were measured

832   in the sera derived from 164 individuals (82 controls; mean age: 69 years; 51M/31F and

833   82 PD subjects: mean age: 67 years; 41M/41F) by ELISA (Mann–Whitney U test; p-

834   value: 0.0004).

835   **Additional material**

836   **Additional file 1. General characteristics of the subjects included in the**

837   **measurement of serum GNPDA2 levels**

838   **Additional file 2. Olfactory proteomics.** Differential expressed proteins between

839   controls, and LTS staging (limbic, early-neocortical, and neocortical stages).

840   **Additional file 3.** Functional analysis of common deregulated proteins across LTS

841   stages.

842   **Additional file 4.** Functional analysis of deregulated OB proteome in each LTS stage.

843   **Additional file 5.** Functional metrics of the differential OB proteome across LTS

844   staging. A) Using Reactome database, differential OB proteomic expression profiles

845   detected across LTS staging were mapped into regulatory pathways (See additional file

846   4 for more details). B) Specific-neuronal functional categories for the differential OB

847   proteomic expression profile detected in each LTS stage (See additional file 4 for more

848   details).

849   **Additional file 6.** Disease and biofunction analysis of differential OB proteomes.

850   **Additional file 7.** CSF samples included in this study.
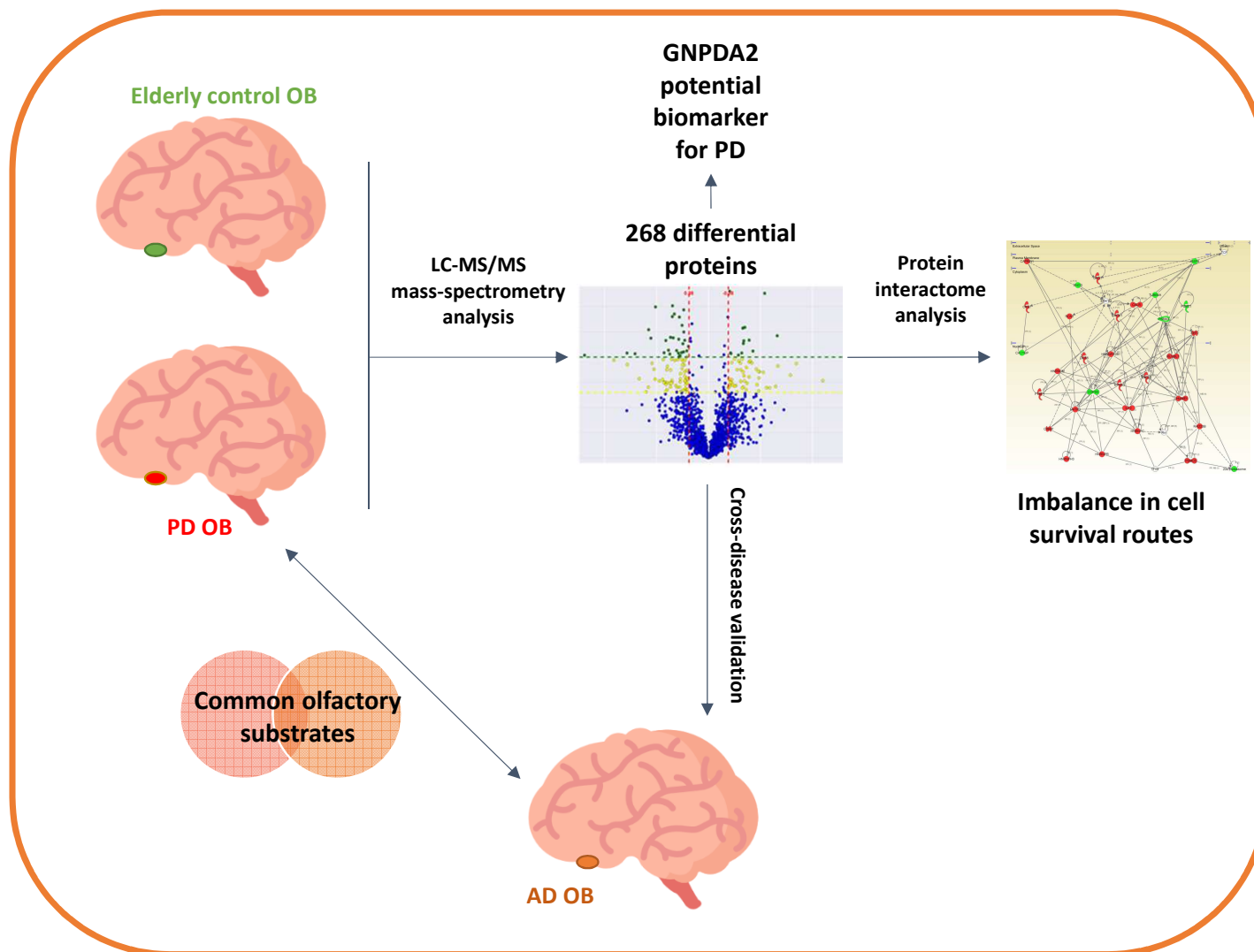
851   **Additional file 8.** Traceability analysis across LTS proteomic datasets.

852   **Additional file 9.** Monitoring of OB survival routes and specific olfactory proteins

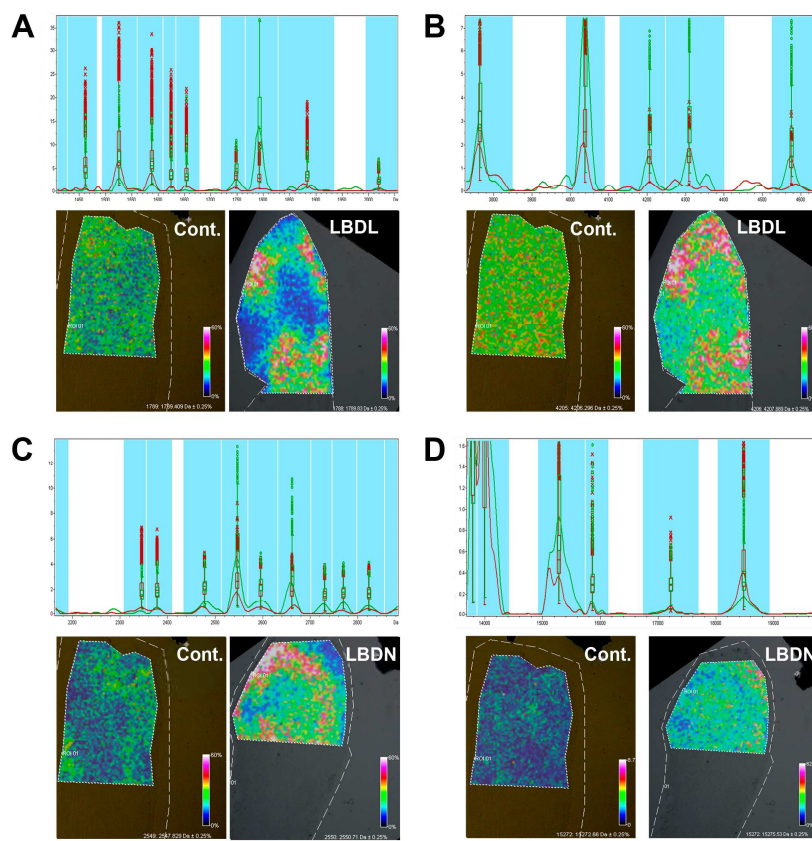853   between PD and AD stages. Confirmation of the GNPDA2 overexpression in the OB of

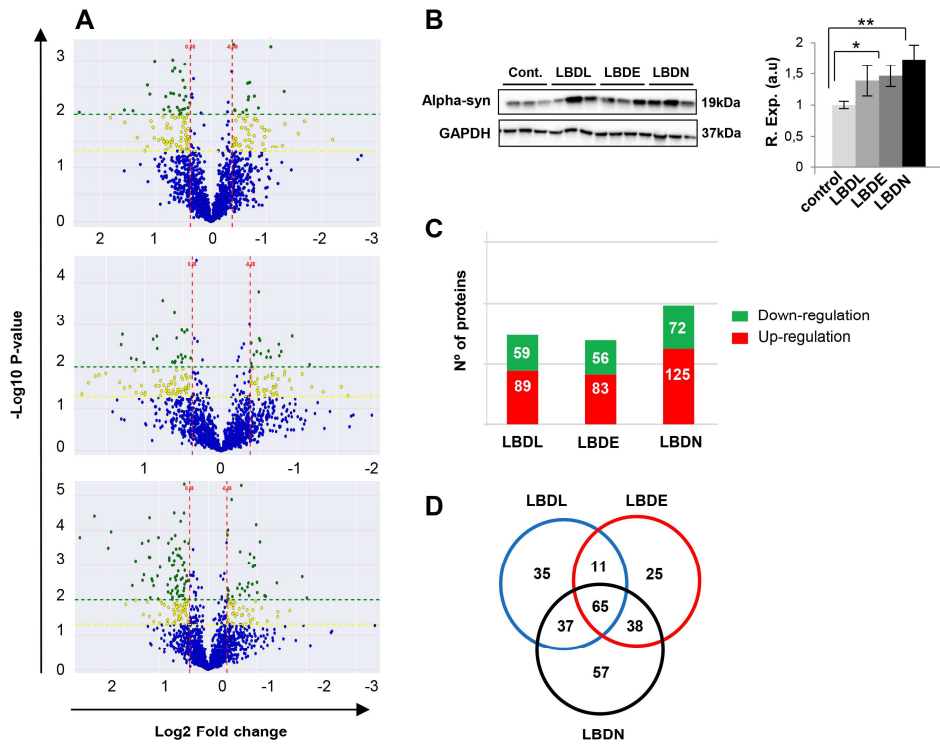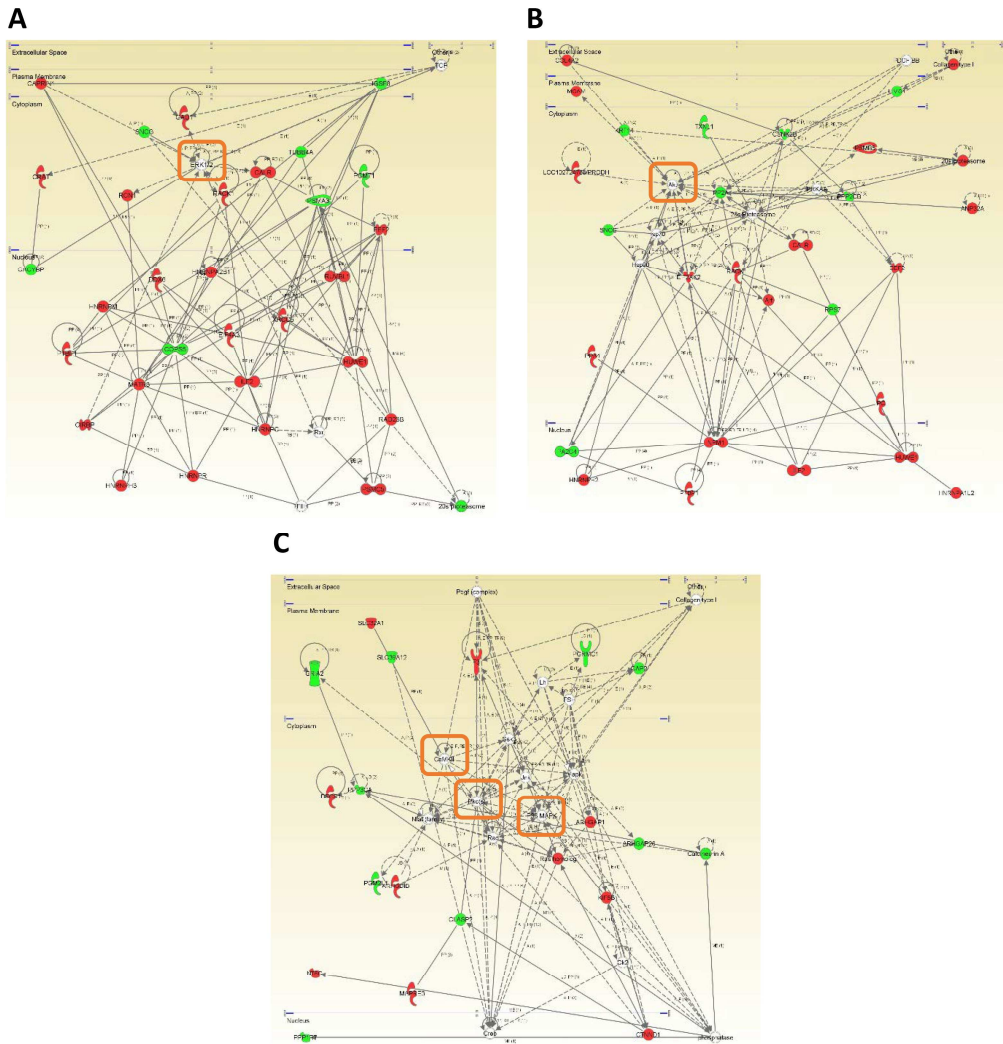854   PD subjects (independent validation).

855

Case	Age	Sex	Clinical diagnosis	Onset	Duration (years)	PMI (hours)	Neuropathological diagnosis
Controls							
C008	93	F				9	ageing-related changes
C048	68	M				10	micro-vascular pathology
C064	63	F				21	cerebellar infarcts
BK-0300	75	F				20	ARP I-II
BK-1378	78	M				6	leucoencephalopathy
BK-1078	84	F				6	Vascular encephalopathy
BK-1195	82	F				8	Acute stroke
BK-1485	79	M				5	Acute stroke
PD							
PD295	83	M	PD	67	16	26	LBDL
PD340	67	M	PD	53	14	12	LBDL
PD356	86	F	PD	75	9	19	LBDL
PD541	72	M	PD	66	6	11	LBDL
PD546	84	F	PD	71	13	25	LBDL
PD579	76	M	PD	55	21	9	LBDL
PD591	77	M	PD	68	9	17	LBDL
PD275	79	M	PD	65	15	22	LBDE
PD354	88	F	PD	77	11	8	LBDE
PD423	66	F	PD	53	13	19	LBDE
PD436	90	M	PD	82	8	14	LBDE
PD520	80	M	PD	56	24	22	LBDE
PD530	85	M	PD	77	8	12	LBDE
PD357	71	M	PD	37	34	15	LBDN
PD450	66	M	PD	47	19	13	LBDN
PD495	88	F	PD	61	28	25	LBDN
PD501	89	F	PD	82	7	16	LBDN
PD537	84	M	PD	84	9	18	LBDN
PD550	83	F	PD	77	7	24	LBDN
PD562	79	M	PD	72	7	16	LBDN
PD636	84	M	PD	65	20	22	LBDN
AD							
1452	70	M	AD	n.a	n.a	3	Braak I
1370	79	F	AD	n.a	n.a	10	Braak II
1429	78	F	AD	n.a	n.a	3	Braak II

1433	62	M	AD	n.a	n.a	9	Braak II
1247	81	M	AD	n.a	n.a	5	Braak III
1517	84	M	AD	n.a	n.a	20	Braak III
1242	82	F	AD	n.a	n.a	17	Braak IV
1248	84	M	AD	n.a	n.a	12	Braak IV
1254	89	M	AD	n.a	n.a	3	Braak IV
CS-1445	73	F	AD	66	7	3	Braak VI
CS-0662	75	M	AD	71	4	4	Braak VI
CS-0535	81	F	AD	70	11	4	Braak VI
CS-0673	75	M	AD	60	15	4	Braak VI
CS-1232	84	M	AD	77	11	5	Braak VI

A

-Log10 P-value

Log2 Fold change

B

Cont.   LBDL   LBDE   LBDN

Alpha-syn   19kDa

GAPDH   37kDa

R. Exp. (a.u)

**   *

control   LBDL   LBDE   LBDN

C

Nº of proteins

Down-regulation
Up-regulation

LBDL   LBDE   LBDN

59   56   72
89   83   125

D

LBDL   LBDE

35   11   25

37   65   38

57

LBDN

A

SCGN
GAPDH

CACYBP
GAPDH

GNPDA2
GAPDH

RACK1
GAPDH

B

α-synuclein

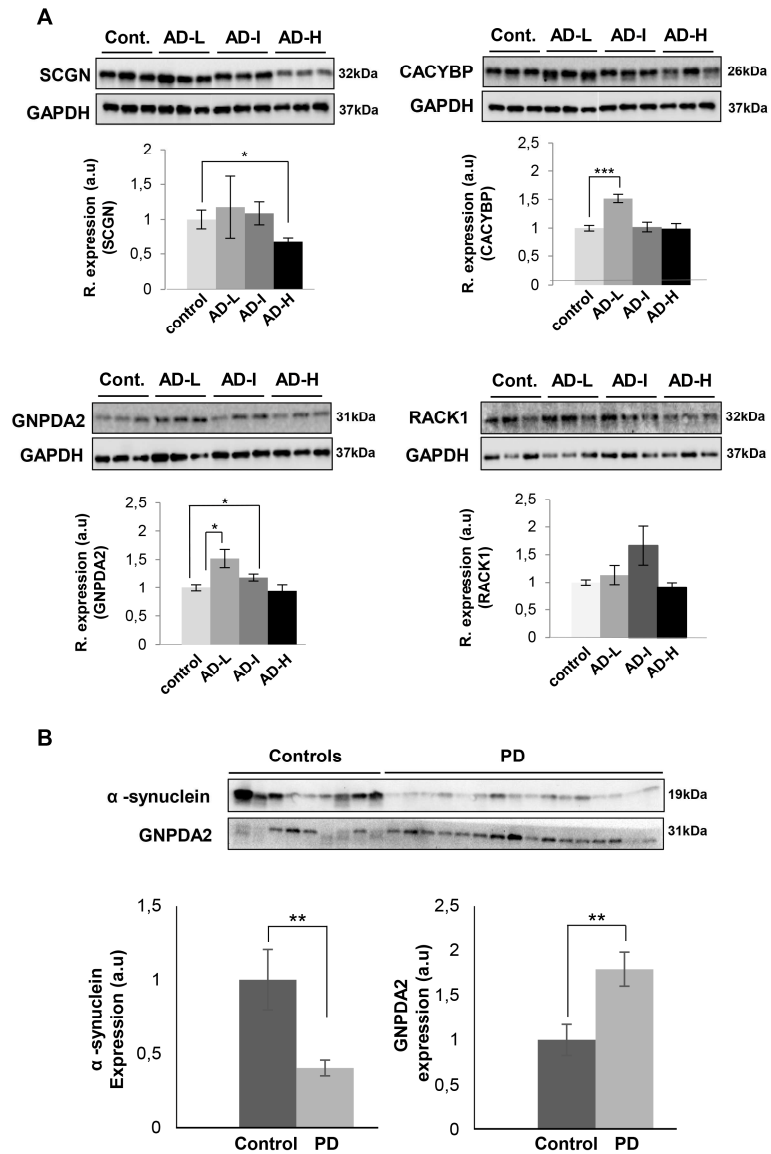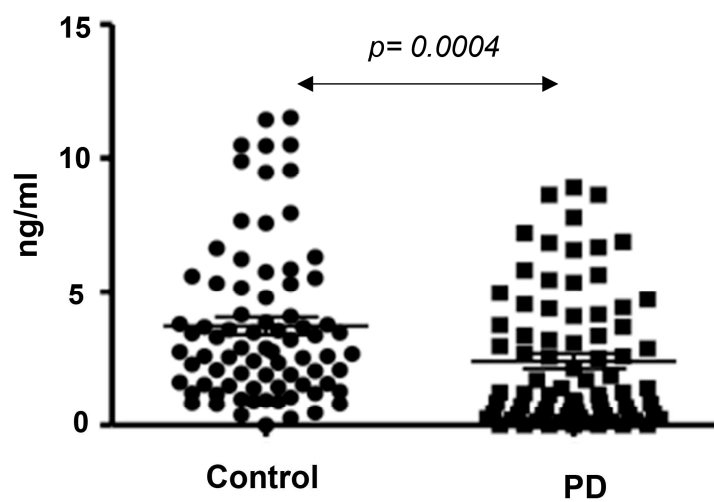GNPDA2
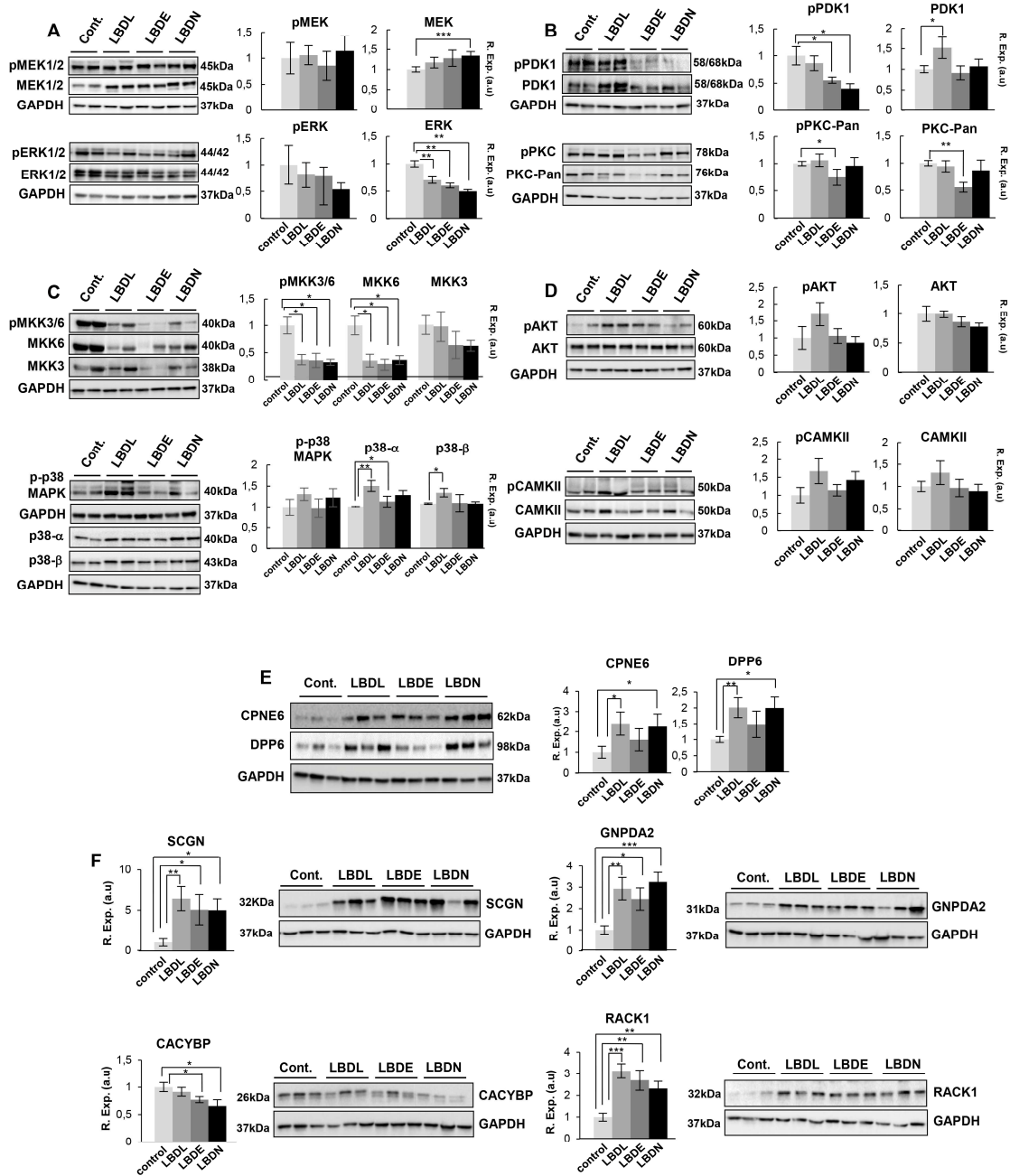
Highlights

- The proteomic profile of postmortem OBs across parkinsonian LTS stages was analyzed

- Two hundred sixty eight proteins were deregulated across LTS staging of PD

- Network-proteomics revealed cell survival signaling imbalance across LTS stages

- Different expression of common olfactory substrates was observed between AD and PD.

- Serum GNPDA2 levels were significantly decreased in PD population